Journal of Sound and Vibration 326 (2009) 221–234

Contents lists available at ScienceDirect

Journal of Sound and Vibration

journal homepage: www.elsevier.com/locate/jsvi

Vibrations of rectangular plates with arbitrary non-uniform elastic edge restraints

X. Zhang, Wen L. Li *

Department of Mechanical Engineering, Wayne State University, 5050 Anthony Wayne Drive, Detroit, MI 48202, USA

ARTICLE INFO

Article history:
Received 11 December 2008
Received in revised form
20 March 2009
Accepted 16 April 2009
Handling Editor: C.L. Morfey
Available online 15 May 2009

ABSTRACT

Arbitrary non-uniform elastic edge restraints represent the most general class of boundary conditions for plate problems, and are encountered in many real-world applications. The vibrations of plates with this kind of boundary conditions, however, are rarely studied in the literature perhaps because there is a lack of suitable analytical or numerical techniques. In this investigation, a general analytical method is derived for the vibration analysis of rectangular plates with elastic edge restraints of varying stiffness. Both rotational and translational restraints can be arbitrarily applied to an edge, and their stiffness distributions are generally described in terms of a set of invariants, cosine functions. The displacement solution is sought simply as a linear combination of several one- and two-dimensional Fourier cosine series expansions. All the unknown Fourier coefficients are treated equally as a set of independent generalized coordinates and solved directly from the Rayleigh–Ritz formulation. Unlike the existing techniques, the current method does not require any special procedures or schemes to deal with different boundary conditions. A few "classical" problems involving non-uniform rotational restraints are first solved and used to check the current solution against some of the existing techniques. The modal results are also presented for plates with more complicated boundary conditions in which an edge is no longer completely restrained in the translational direction. The accuracy and reliability of the current method are repeatedly demonstrated through all these examples.

1. Introduction

There is a wealth of literature about the vibrations of rectangular plates with various boundary conditions, but a vast majority of them is focused on the classical boundary conditions representing various combinations of clamped, simply supported or free edges [1]. While a number of studies have been devoted to the vibrations of plates with uniform elastic restraints along an edge [2–13], few references can be found to deal with non-uniform elastic restraints [14–17]. Many different techniques have been developed for solving the plate problems, which include, but are not limited to, Rayleigh–Ritz procedures, finite strip method [18], superposition method [19], Differential quadrature method (DQ) [15,16,20], and discrete singular convolution method (DSC) [21]. The DQ method was proposed by Bellman [22,23] in the early 1970s. The basic idea in the DQ method is to approximate the derivative of a function as a weighted linear combination of the function values at a number of discrete locations. Thus, any partial differential equation can be reduced to a system of linear algebraic equations. The DQ method has been successfully applied to plate problems by Bert et al. [24]

* Corresponding author. Tel.: +1 313 577 3875.
E-mail address: wli@wayne.edu (W.L. Li).

0022-460X/$ - see front matter © 2009 Elsevier Ltd. All rights reserved.
doi:10.1016/j.jsv.2009.04.021

Nomenclature

a	plate dimension in x direction
A_{mn}	double Fourier series coefficients
b	plate dimension in y direction
c_m^j	single Fourier series coefficients
d_n^j	single Fourier series coefficients
D	flexural rigidity $(= Eh^3/(12(1-\nu^2)))$
E	Young's modulus
h	plate thickness
j	index in the special functions and single Fourier series $(= 1, 2, 3, 4)$
k_{x0}, k_{xa}	translational stiffnesses function at, respectively, $x = 0$ and a
k_{y0}, k_{yb}	translational stiffnesses function at, respectively, $y = 0$ and b
$\mathbf{K}$	stiffness matrix
K_{x0}, K_{xa}	rotational stiffnesses function at, respectively, $x = 0$ and a
K_{y0}, K_{yb}	rotational stiffnesses function at, respectively, $y = 0$ and b
m	Fourier series index in x-direction $(= 0, 1 \ldots M-1)$
M	Fourier series truncation number in x-direction
$\mathbf{M}$	mass matrix
M_x, M_y	bending moment
M_{xy}	twisting moment
n	Fourier series index in y-direction $(= 0, 1 \ldots N-1)$
N	Fourier series truncation number in y-direction
Q_x, Q_y	shear forces
r	aspect ratio $(= a/b)$
$w(x, y)$	flexural displacement
δ_{mn}	Kronecher delta function
λ_{am}	$m\pi/a$
λ_{bn}	$n\pi/b$
ν	Poisson's ratio
ρ	mass density
ω	angular frequency
Ω	dimensionless frequency parameter $(= \omega a^2\sqrt{\rho h/D})$

and Laura and Gutierrez [15]. Despite its certain level of success in solving various physical and engineering problems, the wide applications of this method have been hampered by the uncertainties or controversy with selecting the base functions, grid points and weighting coefficients. Delta-grids are commonly used in approximating the second-order derivatives as included in the boundary conditions of a plate problem. However, such grids can potentially lead to an ill-conditioned weighting coefficient matrix [16]. DSC method was recently developed by Wei [25]. The regularized Shannon's delta kernel is used, and the differentiation is carried out "analytically" on certain discrete points. This method has been applied to the vibrations of plates with mixed and non-uniform edge restraints [17,21]. Although the DSC method has been shown to be highly accurate for simply supported plates with/without rotational restraints, it will lose its high order accuracy at an edge which is not completely restrained in the transverse direction. For instance, a difficulty of accommodating free edges has been considered a pressing issue in the DSC analysis of structures [26]. To overcome this problem, an iteratively matched boundary scheme based on one-sided finite difference was proposed to generate function values at enough fictitious points for the DSC analysis of beams with a free edge [26]. It is not clear whether the mixed use of the finite difference and DSC algorithms will ultimately affect the accuracy of the solution when extended to plates with a transversely-movable edge. Superposition method was proposed by Gorman in solving plate problems under various boundary conditions [19,27–29]. In the superposition method, a general boundary condition is decomposed into a number of simple boundary conditions for which analytical solutions exist or can be easily derived. In using this technique, however, one needs to have a good understanding of the original problems, and customize the solution procedures accordingly to best fit each kind of boundary conditions, which may not be an easy task in view of the variety of possible boundary conditions encountered in practice.

It is commonly believed an exact solution is available only for plates which are simply supported along, at least, one pair of opposite edges, and one has to resort to an approximate solution for other boundary conditions. Rayleigh–Ritz technique is most widely used in finding an approximate solution. For plate problems, the admissible functions used in the Rayleigh–Ritz procedure are often expressed in terms of the beam functions obtained under similar boundary conditions [30–34]. Consequently, a specific set of beam functions is required for each type of boundary conditions. Regardless of other possible issues and concerns, the use of beam functions clearly becomes problematic when the boundary condition or restraint is not uniform along an edge.

Instead of the beam functions, one may also use other forms of admissible functions such as simple or orthogonal polynomials, trigonometric functions and their combinations [12,13,35–42]. When the admissible functions do not form a complete set, the accuracy and convergence of the resulting solution cannot be easily estimated. A well-known problem with use of complete (orthogonal) polynomials is that the higher order polynomials tend to become numerically unstable due to the computer round-off errors. This numerical difficulty can be avoided by using the trigonometric functions or the combinations of trigonometric functions and lower order polynomials. Although it has become a "standard" practice to express the plate displacement function as the series expansion of the beam functions (whether they are in the form of trigonometric functions, hyperbolic functions, polynomials or their combinations), there is no guarantee mathematically that such a representation will actually converge to the true solution because of the difference between the beam and plate boundary conditions. While the limitation of such a mathematical treatment is not readily assessed, its practical

implication becomes immediately clear when a non-uniform boundary condition is specified along an edge. More explicitly, a *similar* boundary condition cannot be readily chosen for the purpose of determining the *appropriate* beam functions.

Hurlebaus et al. [43] proposed a Fourier cosine series solution for calculating the eigenfrequencies and mode shapes for a (composite) plate with *completely free edges*. The exactness of this solution was questioned by Rosales and Filipich [44]. In particular, they insisted that when the uniform convergence of the essential functions (which include the slopes in the plate problem) could not be ensured, there was the probability that the eigenvalue would converge to an approximate value, or even more serious, jump to other eigenvalue (i.e., the loss of eigenvalues). In an earlier paper [45], they developed a variational method, the so-called whole element method (WEM), to calculate the natural frequencies of a free rectangular plate. The displacement solution was expressed in the form of sine series plus a few complementary terms, and the solution was obtained as an extremizing sequence corresponding to the stationarity condition for a functional defined over the domain of the plate. Probably because of the free boundary condition along each edge, the functional they used did not contain any boundary variable or involve any boundary integral. It is a question whether the series solutions derived in Refs. [43,45] can be extended to other boundary conditions than the completely free case.

Recently, an exact Fourier series method was proposed for the in-plane [46] and out-of-plane [47] vibration analysis of plates with uniform elastic restraints along edges. In this method, the Fourier series solution is constructed in such a way that it can be directly differentiated, term-by-term, to derive the uniformly convergent series expansions for all the interested derivatives or variables. Therefore, a solution in strong form can be obtained by letting the series simultaneously satisfy both the governing differential equation and the boundary conditions exactly on a point-wise basis. In this investigation, the Fourier series solution is extended to plates with non-uniform elastic edge restraints. The stiffness for each of the elastic restraints is allowed to vary arbitrarily along an edge. Instead of seeking a solution in strong form as in the previous studies, all the Fourier coefficients will be treated equally and independently as the generalized coordinates and solved directly from the Rayleigh–Ritz technique. Although the size of the final system is increased, the solution procedures are simplified significantly.

2. Vibration of a rectangular plate

The governing differential equation for the free vibration of a plate is given by

$$D\nabla^4 w(x,y) - \rho h\omega^2 w(x,y) = 0 \tag{1}$$

where $\nabla^4 = \partial^4/\partial x^4 + 2\partial^4/\partial x^2\partial y^2 + \partial^4/\partial y^4$, $w(x,y)$ is the flexural displacement, ω is angular frequency, and D, ρ and h are, respectively, the flexural rigidity, the mass density and the thickness of the plate .

In terms of the flexural displacement, the bending and twisting moments, and the transverse shearing forces can be expressed as

$$M_x = -D\left(\frac{\partial^2 w}{\partial x^2} + \nu\frac{\partial^2 w}{\partial y^2}\right), \tag{2}$$

$$M_y = -D\left(\frac{\partial^2 w}{\partial y^2} + \nu\frac{\partial^2 w}{\partial x^2}\right), \tag{3}$$

$$M_{xy} = -D(1-\nu)\frac{\partial^2 w}{\partial x\partial y}, \tag{4}$$

$$Q_x = -D\frac{\partial}{\partial x}(\nabla^2 w) + \frac{\partial M_{xy}}{\partial y} = -D\left(\frac{\partial^3 w}{\partial x^3} + (2-\nu)\frac{\partial^3 w}{\partial x\partial y^2}\right), \tag{5}$$

and

$$Q_y = -D\frac{\partial}{\partial y}(\nabla^2 w) + \frac{\partial M_{xy}}{\partial x} = -D\left(\frac{\partial^3 w}{\partial y^3} + (2-\nu)\frac{\partial^3 w}{\partial x^2\partial y}\right). \tag{6}$$

The boundary conditions for an elastically restrained rectangular plate are as follows:

$$k_{x0}(y)w = Q_x, \quad K_{x0}(y)\partial w/\partial x = -M_x, \quad \text{at } x = 0 \tag{7, 8}$$

$$k_{xa}(y)w = -Q_x, \quad K_{xa}(y)\partial w/\partial x = M_x, \quad \text{at } x = a \tag{9, 10}$$

$$k_{y0}(x)w = Q_y, \quad K_{y0}(x)\partial w/\partial y = -M_y, \quad \text{at } y = 0 \tag{11,12}$$

and

$$k_{yb}(x)w = -Q_y, \quad K_{yb}(x)\partial w/\partial y = M_y, \quad \text{at } y = b \tag{13,14}$$

where $k_{x0}(y)$ and $k_{xa}(y)$ ($k_{y0}(x)$ and $k_{yb}(x)$) are the stiffness functions for the translational elastic restraints, and $K_{x0}(y)$ and $K_{xa}(y)$ ($K_{y0}(x)$ and $K_{yb}(x)$) are the stiffness functions for the rotational restraints at $x=0$ and $x=a$ ($y=0$ and $y=b$), respectively. It should be noted that the stiffness functions can be arbitrarily specified along any edge. Eqs. (7)–(14) represent a set of general boundary conditions for a plate, and all the familiar classical homogenous boundary conditions can be considered as the special cases when the stiffness functions are uniformly specified as zero or infinity along each edge.

As in the previous study [47], the displacement solution will be sought as a series expansion in the form of

$$w(x,y)=\sum_{m=0}^{\infty}\sum_{n=0}^{\infty}A_{mn}\cos\lambda_{am}x\cos\lambda_{bn}y+\sum_{j=1}^{4}\left(\xi_b^j(y)\sum_{m=0}^{\infty}c_m^j\cos\lambda_{am}x+\xi_a^j(x)\sum_{n=0}^{\infty}d_n^j\cos\lambda_{bn}y\right) \tag{15}$$

where $\lambda_{am}=m\pi/a$, $\lambda_{bn}=n\pi/b$, and $\xi_a^j(x)$ (or $\xi_b^j(y)$) represent a set of closed-form supplementary functions, for example, defined as

$$\xi_a^1(x)=\frac{9a}{4\pi}\sin\left(\frac{\pi x}{2a}\right)-\frac{a}{12\pi}\sin\left(\frac{3\pi x}{2a}\right),\quad \xi_a^2(x)=-\frac{9a}{4\pi}\cos\left(\frac{\pi x}{2a}\right)-\frac{a}{12\pi}\cos\left(\frac{3\pi x}{2a}\right), \tag{16,17}$$

$$\xi_a^3(x)=\frac{a^3}{\pi^3}\sin\left(\frac{\pi x}{2a}\right)-\frac{a^3}{3\pi^3}\sin\left(\frac{3\pi x}{2a}\right),\quad \xi_a^4(x)=-\frac{a^3}{\pi^3}\cos\left(\frac{\pi x}{2a}\right)-\frac{a^3}{3\pi^3}\cos\left(\frac{3\pi x}{2a}\right). \tag{18,19}$$

It is easy to verify that $\xi_a'^1(0)=\xi_a'^2(a)=\xi_a'''^3(0)=\xi_a'''^4(a)=1$, and all the other first and third derivatives are identically equal to zero along the edges. By choosing the supplementary functions in such a way, each of the 1-D Fourier series expansions in Eq. (15) will now have a simple explanation; that is, it represents either the first or the third derivative of the displacement function along one of the edges. As a result, the 2-D series simply represent a residual displacement field which is periodic and adequately smooth over the entire x–y domain. More importantly, it is now guaranteed to uniformly converge at a substantially improved speed for any boundary condition [47,48].

In Ref. [47], the series solution is sought in strong form by simultaneously satisfying both the governing differential equation and the boundary conditions exactly on a point-wise basis. Because the series expansions will have to be truncated in numerical calculations, the exactness of the solution should be understood as *a solution with arbitrary precision*. A similar solution can also be obtained for the current plate problems involving arbitrary non-uniform edge supports. In this study, however, the solution will be sought in weak form using the Rayleigh–Ritz procedure. Accordingly, all the Fourier coefficients will be considered as mutually independent generalized coordinates, and solved directly from, for instance, the Hamilton's equation

$$\delta\int_{t_0}^{t_1}(T-V)\,\mathrm{d}t=0 \tag{20}$$

where T is the total kinetic energy and V is the total potential energy.

For a purely bending plate, the total potential energy can be expressed as

$$\begin{aligned}V=&\frac{D}{2}\int_0^a\int_0^b[(\partial^2w/\partial x^2)^2+(\partial^2w/\partial y^2)^2+2\nu\partial^2w/\partial x^2\partial^2w/\partial y^2+2(1-\nu)(\partial^2w/\partial x\partial y)^2]\,\mathrm{d}x\,\mathrm{d}y\\&+\frac{1}{2}\int_0^b(k_{x0}w^2+K_{x0}(\partial w/\partial x)^2)_{x=0}\,\mathrm{d}y+1/2\int_0^b(k_{xa}w^2+K_{xa}(\partial w/\partial x)^2)_{x=a}\,\mathrm{d}y\\&+\frac{1}{2}\int_0^a(k_{y0}w^2+K_{y0}(\partial w/\partial y)^2)_{y=0}\,\mathrm{d}x+1/2\int_0^a(k_{ya}w^2+K_{ya}(\partial w/\partial y)^2)_{y=b}\,\mathrm{d}x\end{aligned} \tag{21}$$

and the total kinetic energy is calculated from

$$T=\frac{1}{2}\int_0^a\int_0^b\rho h(\partial w/\partial t)^2\,\mathrm{d}x\,\mathrm{d}y. \tag{22}$$

In Eq. (21), the first integral represents the strain energy due to the bending of the plate, and the remaining integrals represent the potential energies resulting from the deflections of the elastic constraints.

In order to derive the final system against all the unknown Fourier coefficients, one has to substitute the displacement expression, Eq. (15), into the Hamilton's equation, Eq. (20), and calculate partial derivatives with respect to each of Fourier coefficients. For example, the first term of the bending energy term, after differentiated with respect to A_{mn}, can be

written as

$$\begin{aligned}
&\frac{\partial}{\partial A_{mn}}\left[\frac{D}{2}\int_0^a\int_0^b(\partial^2 w/\partial x^2)^2\,\mathrm{d}x\,\mathrm{d}y\right]\\
&=\frac{D}{2}\int_0^a\int_0^b\frac{\partial}{\partial A_{mn}}(\partial^2 w/\partial x^2)^2\,\mathrm{d}x\,\mathrm{d}y=\frac{D}{2}\int_0^a\int_0^b 2\partial^2 w/\partial x^2(-\lambda_{am}^2)\cos\,\lambda_{am}x\,\cos\,\lambda_{bn}y\,\mathrm{d}x\,\mathrm{d}y\\
&=\lambda_{am}^2 D\int_0^a\int_0^b\sum_{m'=0}^{\infty}\sum_{n'=0}^{\infty}\lambda_{am'}^2 A_{m'n'}\,\cos\,\lambda_{am'}x\,s\lambda_{bn'}y\,\cos\,\lambda_{am}x\,\cos\,\lambda_{bn}y\,\mathrm{d}x\,\mathrm{d}y\\
&\quad+\lambda_{am}^2 D\int_0^a\int_0^b\sum_{j=1}^{4}\xi_b^j(y)\sum_{m'=0}^{\infty}(\lambda_{am'}^2 c_{m'}^j\,\cos\,\lambda_{am'}x)\,\cos\,\lambda_{am}x\,\cos\,\lambda_{bn}y\,\mathrm{d}x\,\mathrm{d}y\\
&\quad-\lambda_{am}^2 D\int_0^a\int_0^b\sum_{j=1}^{4}\xi_a''^j(x)\sum_{n'=0}^{\infty}(d_{n'}^j\cos\lambda_{bn'}y)\cos\,\lambda_{am}x\,\cos\,\lambda_{bn}y\,\mathrm{d}x\,\mathrm{d}y\\
&\quad=D\left[\lambda_{am}^4\left(A_{mn}+\sum_{j=1}^{4}\tilde{\beta}_n^j c_m^j\right)-\lambda_{am}^2\sum_{j=1}^{4}\tilde{\tilde{\alpha}}_m^j d_n^j\right]\Delta_m\Delta_n
\end{aligned}\tag{23}$$

where $\Delta_m=\int_0^a(\cos\,\lambda_{am}x)^2\,\mathrm{d}x=(1+\delta_{m0})a/2$, $\Delta_n=\int_0^b(\cos\,\lambda_{bn}y)^2\,\mathrm{d}y=(1+\delta_{n0})b/2$, $\tilde{\beta}_n^j=1/\Delta_n\int_0^b\xi_b^j(y)\cos\,\lambda_{bn}y\,\mathrm{d}y$, and $\tilde{\tilde{\alpha}}_m^j=1/\Delta_m\int_0^a\xi_a''^j(x)\cos\,\lambda_{am}x\,\mathrm{d}x$. The detailed calculations are given in Appendix A.

As mentioned earlier, in this study the stiffness for each elastic restraint can be arbitrarily specified along an edge. To unify the calculations, every stiffness function, such as $k_{x0}(y)$, will be expanded into Fourier series as

$$k_{x0}(y)=\sum_{l=0}^{\infty}\tilde{k}_{x0,l}\,\cos\left(\frac{l\pi}{b}y\right)\tag{24}$$

For any given continuous stiffness function, the series expansion in Eq. (24) will converge at a rate of, at least, $(l\pi)^2$. Accordingly, the contribution from this boundary restraint can be calculated as

$$\begin{aligned}
&\frac{\partial}{\partial A_{mn}}\left[\frac{1}{2}\int_0^b k_{x0}(y)w^2 0,(0,y)\,\mathrm{d}y\right]\\
&=\frac{1}{2}\int_0^b k_{x0}(y)\frac{\partial}{\partial A_{mn}}[w^2(0,y)]\,\mathrm{d}y=\int_0^b k_{x0}(y)w(0,y)\cos(\lambda_{bn}y)\,\mathrm{d}y\\
&=\int_0^b k_{x0}(y)\left\{\sum_{m'=0}^{\infty}\sum_{n'=0}^{\infty}A_{m'n'}\,\cos\,\lambda_{bn'}y+\sum_{j=1}^{4}\left[\xi_b^j(y)\sum_{m'=0}^{\infty}c_{m'}^j+\xi_a^j(0)\sum_{n'=0}^{\infty}d_{n'}^j\,\cos\,\lambda_{bn'}y\right]\right\}\cos\,\lambda_{bn}y\,\mathrm{d}y\\
&=\frac{1}{2}\sum_{m'=0}^{\infty}\sum_{n'=0}^{\infty}A_{m'n'}\int_0^b k_{x0}(y)(\cos\,\lambda_{b(n+n')}y+\cos\,\lambda_{b(n-n')}y)\,\mathrm{d}y\\
&\quad+\frac{1}{2}\sum_{j=1}^{4}\sum_{n'=0}^{\infty}\xi_a^j(0)d_{n'}^j\int_0^b k_{x0}(y)(\cos\,\lambda_{b(n+n')}y+\cos\,\lambda_{b(n-n')})\,\mathrm{d}y\\
&\quad+\sum_{j=1}^{4}\int_0^b\xi_b^j(y)k_{x0}(y)\cos\,\lambda_{bn}y\,\mathrm{d}y\sum_{m'=0}^{\infty}c_{m'}^j\\
&=\frac{1}{2}\sum_{m'=0}^{\infty}\sum_{n'=0}^{\infty}(\tilde{k}_{x0,n+n'}+\tilde{k}_{x0,|n-n'|})A_{m'n'}\\
&\quad+\frac{1}{2}\sum_{j=1}^{4}\left[\sum_{l=0}^{\infty}k_{x0,l}(\tilde{\beta}_{n+l}^j+\tilde{\beta}_{|n-l|}^j)\sum_{m'=0}^{\infty}c_{m'}^j+\sum_{n'=0}^{\infty}\xi_a^j(0)(\tilde{k}_{x0,n+n'}+\tilde{k}_{x0,|n-n'|})d_{n'}^j\right]
\end{aligned}\tag{25}$$

When a (number of) discrete restraint(s) is applied along an edge, the corresponding stress function can be expressed in terms of delta function(s). Consequently, the series representation as in Eq. (24) may not be preferred because of the possible convergence problem at the discontinuity location(s). In such a case, however, the integrals in Eq. (25) can be readily calculated by making use of the characteristic of a delta function.

By accounting for all the other terms in Eqs. (21) and (22), a set of linear algebraic equations (resulting from the derivatives with respect to A_{mn}) can be derived as

$$
\begin{aligned}
&D[\lambda_{am}^4+\lambda_{bn}^4+2\lambda_{am}^2\lambda_{bn}^2]\Delta_m\Delta_n A_{mn}\\
&+\frac{1}{2}\sum_{n'=0}^{\infty}\sum_{m'=0}^{\infty}(\tilde{k}_{x0,n+n'}+\tilde{k}_{x0,|n-n'|}+(-1)^{m'+m}(\tilde{k}_{xa,n+n'}+\tilde{k}_{xa,|n-n'|}))A_{m'n'}\\
&+\frac{1}{2}\sum_{m'=0}^{\infty}\sum_{n'=0}^{\infty}(\tilde{k}_{y0,m+m'}+\tilde{k}_{y0,|m-m'|}+(-1)^{n'+n}(\tilde{k}_{yb,m+m'}+\tilde{k}_{yb,|m-m'|}))A_{m'n'}\\
&+\sum_{j=1}^{4}D[(\lambda_{am}^4+\nu\lambda_{am}^2\lambda_{bn}^2)\beta_n^j-(\lambda_{bn}^2+\nu\lambda_{am}^2)\bar{\beta}_n^j-2(1-\nu)\lambda_{bn}\lambda_{am}^2\bar{\beta}_n^j]\Delta_m\Delta_n c_m^j\\
&+\frac{1}{2}\sum_{j=1}^{4}\sum_{l=0}^{\infty}\sum_{m'=0}^{\infty}(k_{x0,l}+k_{xa,l}(-1)^{m+m'})(\tilde{\beta}_{n+l}^j+\tilde{\beta}_{|n-l|}^j)c_{m'}^j\\
&+\frac{1}{2}\sum_{j=1}^{4}\sum_{m'=0}^{\infty}[\xi_b^j(0)(\tilde{k}_{y0,m+m'}+\tilde{k}_{y0,|m-m'|})+\xi_b^j(b)(-1)^n(\tilde{k}_{yb,m+m'}+\tilde{k}_{yb,|m-m'|})]c_{m'}^j\\
&+\sum_{j=1}^{4}D[(\lambda_{bn}^4+\nu\lambda_{bn}^2\lambda_{am}^2)\alpha_m^j-(\lambda_{am}^2+\nu\lambda_{bn}^2)\bar{\alpha}_m^j-2(1-\nu)\lambda_{am}\lambda_{bn}^2\bar{\alpha}_m^j]\Delta_m\Delta_n d_n^j\\
&+\frac{1}{2}\sum_{j=1}^{4}\sum_{s=0}^{\infty}\sum_{n'=0}^{\infty}(k_{y0,s}+(-1)^{n+n'}k_{yb,s})(\tilde{\alpha}_{m+s}^j+\tilde{\alpha}_{|m-s|}^j)d_{n'}^j\\
&+\frac{1}{2}\sum_{j=1}^{4}\sum_{n'=0}^{\infty}[\xi_a^j(0)(\tilde{k}_{x0,n+n'}+\tilde{k}_{x0,|n-n'|})+(-1)^m\xi_a^j(a)(\tilde{k}_{xa,n+n'}+\tilde{k}_{xa,|n-n'|})]d_{n'}^j\\
&-\rho h\omega^2\left[A_{mn}+\sum_{j=1}^{4}\beta_n^j c_m^j+\sum_{j=1}^{4}\alpha_m^j d_n^j\right]\Delta_m\Delta_n=0
\end{aligned}
\tag{26}
$$

where $\xi_b^{\prime\prime j}(y)=\sum_{n=0}^{\infty}\bar{\beta}_n^j\cos\lambda_{bn}y$, and $\xi_a^j(x)=\sum_{n=0}^{\infty}\alpha_m^j\cos\lambda_{am}x$.

Taking partial derivative respect to c_m^i ($i=1,2,3,4$) results in

$$
\begin{aligned}
&\sum_{n'=0}^{\infty}D[(\lambda_{am}^4+\nu\lambda_{am}^2\lambda_{bn}^2)\beta_{n'}^i-(\lambda_{bn'}^2+\nu\lambda_{am}^2)\bar{\beta}_{n'}^i-2(1-\nu)\lambda_{am}^2\lambda_{bn'}\bar{\beta}_n^i]\Delta_m\Delta_{n'}A_{m,n'}\\
&+\frac{1}{2}\sum_{l=0}^{\infty}\sum_{n'=0}^{\infty}\sum_{m'=0}^{\infty}(k_{x0,l}+k_{xa,l}(-1)^{m'+m})(\tilde{\beta}_{n'+l}^i+\tilde{\beta}_{|n'-l|}^i)A_{m',n'}\\
&+\frac{1}{2}\sum_{m'=0}^{\infty}\sum_{n'=0}^{\infty}(\xi_b^i(0)(\tilde{k}_{y0,m+m'}+\tilde{k}_{y0,|m-m'|})+\xi_b^i(b)(-1)^{n'}(\tilde{k}_{yb,m+m'}+\tilde{k}_{yb,|m-m'|}))A_{m',n'}\\
&+\sum_{j=1}^{4}D[\lambda_{am}^4\beta_{i,j}^{0,0}+\beta_{i,j}^{2,2}-\nu\lambda_{am}^2(\beta_{i,j}^{2,0}+\beta_{i,j}^{0,2})+2(1-\nu)\lambda_{am}^2\beta_{i,j}^{1,1}]\Delta_m c_m^j\\
&+\sum_{j=1}^{4}\sum_{l=0}^{\infty}\sum_{m'=0}^{\infty}(k_{x0,l}+k_{xa,l}(-1)^{m+m'})\beta_{i,j,l}^{0,0}c_{m'}^j\\
&+\frac{1}{2}\sum_{j=1}^{4}\sum_{m'=0}^{\infty}[\xi_b^i(0)\xi_b^j(0)(\tilde{k}_{y0,m+m'}+\tilde{k}_{y0,|m-m'|})+\xi_b^i(b)\xi_b^j(b)(\tilde{k}_{yb,m+m'}+\tilde{k}_{yb,|m-m'|})]c_{m'}^j\\
&+\frac{1}{2}\sum_{j=1}^{4}\sum_{m'=0}^{\infty}[\xi_b'^i(0)\xi_b'^j(0)(\tilde{K}_{y0,m+m'}+\tilde{K}_{y0,|m-m'|})+\xi_b'^i(b)\xi_b'^j(b)(\tilde{K}_{yb,m+m'}+\tilde{K}_{yb,|m-m'|})]c_{m'}^j\\
&+\sum_{j=1}^{4}\sum_{n'=0}^{\infty}D[-\lambda_{am}^2\bar{\alpha}_m^j\beta_{n'}^i-\lambda_{bn'}^2\alpha_m^j\bar{\beta}_{n'}^i+\nu\bar{\alpha}_m^j\bar{\beta}_{n'}^i+\nu\lambda_{am}^2\lambda_{bn'}^2\beta_{n'}^i\alpha_m^j+2(1-\nu)\lambda_{am}\lambda_{bn'}\bar{\beta}_{n'}^i\bar{\alpha}_m^j]\Delta_m\Delta_{n'}d_{n'}^j\\
&+\frac{1}{2}\sum_{j=1}^{4}\sum_{l=0}^{\infty}\sum_{n'=0}^{\infty}(k_{x0,l}\xi_a^j(0)+k_{xa,l}(-1)^m\xi_a^j(a))(\tilde{\beta}_{n'+l}^i+\tilde{\beta}_{|n'-l|}^i)d_{n'}^j\\
&+\frac{1}{2}\sum_{j=1}^{4}\sum_{s=0}^{\infty}\sum_{n'=0}^{\infty}(k_{y0,s}\xi_b^i(0)+k_{yb,s}(-1)^{n'}\xi_b^i(b))(\tilde{\alpha}_{m+s}^j+\tilde{\alpha}_{|m-s|}^j)d_{n'}^j\\
&-\rho h\omega^2\left[\sum_{n'=0}^{\infty}\left(A_{mn'}+\sum_{j=1}^{4}\alpha_{jm}d_{n'}^j\right)\Delta_m\Delta_{n'}\beta_{n'}^i+\sum_{j=1}^{4}\beta_{i,j}^{0,0}\Delta_m c_m^j\right]=0
\end{aligned}
\tag{27}
$$

Taking partial derivative respect to d_n^i ($i = 1, 2, 3, 4$) results in,

$$\begin{aligned}
&\sum_{m'=0}^{\infty} D[(\lambda_{bn}^4 + \nu\lambda_{bn}^2\lambda_{am'}^2)\alpha_{m'}^i - (\lambda_{am'}^2 + \nu\lambda_{bn}^2)\bar{\bar{\alpha}}_{m'}^i - 2(1-\nu)\lambda_{bn}^2\lambda_{am'}\bar{\alpha}_{m'}^i]\Delta_{m'}\Delta_n A_{m'n} \\
&+\frac{1}{2}\sum_{s=0}^{\infty}\sum_{m'=0}^{\infty}\sum_{n'=0}^{\infty}(k_{y0,s} + k_{yb,s}(-1)^{n'+n})(\tilde{\alpha}_{m'+s}^i + \tilde{\alpha}_{|m'-s|}^i)A_{m'n'} \\
&+\frac{1}{2}\sum_{n'=0}^{\infty}\sum_{m'=0}^{\infty}[\xi_a^i(0)(\tilde{k}_{x0,n+n'} + \tilde{k}_{x0,|n-n'|}) + \xi_a^i(a)(-1)^{m'}(\tilde{k}_{xa,n+n'} + \tilde{k}_{xa,|n-n'|})]A_{m'n'} \\
&+\sum_{j=1}^{4}\sum_{m'=0}^{\infty} D[-\lambda_{bn}^2\bar{\beta}_n^j\alpha_{m'}^i - \lambda_{am'}^2\beta_n^j\bar{\alpha}_{m'}^i + \nu\bar{\beta}_n^j\bar{\alpha}_{m'}^i + \nu\lambda_{bn}^2\lambda_{am'}^2\alpha_{m'}^i\beta_n^j + 2(1-\nu)\lambda_{bn}\lambda_{am'}\bar{\alpha}_{m'}^i\bar{\beta}_n^j]\Delta_{m'}\Delta_n c_{m'}^j \\
&+\frac{1}{2}\sum_{j=1}^{4}\sum_{l=0}^{\infty}\sum_{m'=0}^{\infty}(k_{x0,l}\xi_a^i(0) + k_{xa,l}(-1)^{m'}\xi_a^i(a))(\tilde{\beta}_{n+l}^j + \tilde{\beta}_{|n-l|}^j)c_{m'}^j \\
&+\frac{1}{2}\sum_{j=1}^{4}\sum_{s=0}^{\infty}\sum_{m'=0}^{\infty}(k_{y0,s}\xi_b^j(0) + k_{yb,s}(-1)^n\xi_b^j(b))(\tilde{\alpha}_{m'+s}^i + \tilde{\alpha}_{|m'-s|}^i)c_{m'}^j \\
&+\sum_{j=1}^{4} D[\lambda_{bn}^4\alpha_{i,j}^{0,0} + \alpha_{i,j}^{2,2} - \nu\lambda_{bn}^2(\alpha_{i,j}^{2,0} + \alpha_{i,j}^{0,2}) + 2(1-\nu)\lambda_{bn}^2\alpha_{i,j}^{1,1}]\Delta_n d_n^j \\
&+\sum_{j=1}^{4}\sum_{s=0}^{\infty}\sum_{n'=0}^{\infty}(k_{y0,s} + k_{yb,s}(-1)^{n+n'})\alpha_{i,j,s}^{0,0}d_n^j \\
&+\frac{1}{2}\sum_{j=1}^{4}\sum_{n'=0}^{\infty}[\xi_a^i(0)\xi_a^j(0)(\tilde{k}_{x0,n+n'} + \tilde{k}_{x0,|n-n'|}) + \xi_a^i(a)\xi_a^j(a)(\tilde{k}_{xa,n+n'} + \tilde{k}_{xa,|n-n'|})]d_{n'}^j \\
&+\frac{1}{2}\sum_{j=1}^{4}\sum_{n'=0}^{\infty}[\xi_a'^i(0)\xi_a'^j(0)(\tilde{K}_{x0,n+n'} + \tilde{K}_{x0,|n-n'|}) + \xi_a'^i(a)\xi_a'^j(a)(\tilde{K}_{xa,n+n'} + \tilde{K}_{xa,|n-n'|})]d_{n'}^j \\
&-\rho h\omega^2\left[\sum_{m'=0}^{\infty}\left(A_{m'n} + \sum_{j=1}^{4}\beta_n^j c_{m'}^j\right)\Delta_{m'}\Delta_n\alpha_{m'}^i + \sum_{j=1}^{4}\alpha_{i,j}^{0,0}\Delta_n d_n^j\right] = 0
\end{aligned} \tag{28}$$

Eqs. (26)–(28) can be combined together in more concise matrix form as

$$\left(\mathbf{K} - \frac{\rho h\omega^2}{D}\mathbf{M}\right)\mathbf{a} = 0 \tag{29}$$

where $\mathbf{a} = [A_{01}A_{11}\cdots A_{M1}\cdots A_{0N}A_{1N}\cdots A_{MN}c_0^1c_1^1c_2^1\cdots c_M^1\cdots c_0^4c_1^4c_2^4\cdots c_M^4d_0^1d_1^1d_2^1\cdots d_N^1\cdots d_0^4d_1^4d_2^4\cdots d_N^4]^{\mathrm{T}}$.

It has been assumed in Eq. (29) that all series expansions have been truncated to $m = 0,1,2,\ldots,M$ and $n = 0,1,2,\ldots,N$ for the sake of numerical calculations.

In comparison with the strong form of solution as derived in Ref. [47], the number of equations in the final system is increased by $4(M+N+2)$ since the Fourier coefficients in the 1-D series expansions are considered as independent variables. However, the current solution process is significantly simplified because the restraint equations, in the form of boundary conditions, between the boundary and field Fourier coefficients are no longer explicitly reinforced. However, this does not necessarily imply a loss of the accuracy by the current solution. As a matter of fact, since the solution constructed in Eq. (15) is as smooth as what a classical solution would be required (that is, to belong to $\mathbb{C}^3$ for $\forall(x, y)\in D$: $[0, a]\otimes[0, b]$), the weak and strong formulations can be proved mathematically to be equivalent to each other.

Eq. (29) represents a standard matrix characteristic equation from which all the eigenpairs can be easily determined. Once the Fourier coefficient eigenvector $\mathbf{a}$ is determined for a given eigenvalue, the corresponding mode shape can be constructed directly from the displacement expression, Eq. (15). Even though this study is focused on the free vibrations of an elastically restrained plate, the forced vibration can be readily calculated by simply adding a load vector to the right side of Eq. (29).

3. Results and discussions

Several examples involving plates with non-uniform elastic restraints will be given in this section. First, let us consider a problem previously investigated by several researchers [14–17]. As shown in Fig. 1, it involves a simply supported plate with rotational restraints of parabolically varying stiffness along two opposite edges (SESE). This is a special case of the general boundary conditions, Eqs. (7)–(14), when the stiffness functions are set as: $k_{x0}(y) = k_{xa}(y) = k_{y0}(x) = k_{yb}(x) = \infty$

and $K_{x0}(y) = K_{xa}(y) = 0$, and $K_{y0}(x) = K_{yb}(x) = K_c(1-x)xD/a$ where K_c is a constant. Another "classical" case is referred to as CECE where the two simply supported edges become fully clamped, namely, $K_{x0}(y) = K_{xa}(y) = \infty$. The fundamental frequencies calculated using various methods are shown in Table 1 for both cases. It is noted that the current results compare well with those previously obtained from other different techniques. As mentioned earlier, the series expansion, Eq. (29), will has to be truncated in numerical calculations. The CECE case with $K_c = 1$ is used to examine the convergence of the current solution. As shown in Table 2, the first six frequency parameters become quickly converged at $M = N = 10$ for the given 5-digit precision. For simplicity, the displacement expansion will be truncated to $M = N = 10$ in all the subsequent calculations. More results for other restraining schemes are shown in Table 3 together with those previously obtained by Zhao and Wei [17] using the DSC method. A good agreement is observed between the two different methods.

Although non-uniform restraints against rotations are allowed in the above examples, the transverse displacement is fully restrained along each edge. In many practical applications, however, both the translational and rotational restraints may have to be considered as elastic and their stiffnesses can vary from point to point on an edge. While the restraining of transverse displacement along each edge may be needed in the previous studies for whatever reasons, it is definitely not a

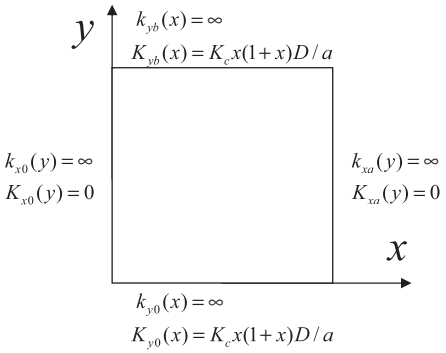

Fig. 1. A simply supported plate with rotational springs of parabolically varying stiffness along two opposite edges, where K_c is a constant.

Table 1
The fundamental frequency parameters, $\Omega = \omega a^2\sqrt{\rho h/D}$, for (a) SESE: Simply supported plate with rotational springs of parabolically varying stiffness along two opposite edges (b) CECE: Setup (a) with two simply supported edges clamped.

λ	SESE						CECE				
	K_c	a	b	c	d	Current	a	b	c	d	Current
0.5	0	12.337	12.34	12.337	12.337	12.349	23.814	23.82	23.816	23.816	23.816
	0.1	12.341	12.34	12.341	12.340	12.354	23.844	23.82	23.818	23.819	23.818
	1	12.372	12.38	12.379	12.362	12.391	23.876	23.85	23.839	23.843	23.839
	10	12.621	12.66	12.666	12.550	12.674	24.136	24.01	23.996	24.019	23.996
	100	13.319	13.37	13.364	13.207	13.366	24.561	24.41	24.393	24.410	24.393
	10^6	13.688	13.7	13.686	13.686	13.686	24.566	24.60	24.578	24.579	24.578
1	0	19.739	19.74	19.734	19.739	19.748	28.951	28.96	28.951	28.952	28.951
	0.1	19.757	19.76	19.761	19.764	19.770	28.969	28.98	28.966	28.970	28.966
	1	19.915	19.95	19.951	19.985	19.960	28.219	29.12	29.102	29.128	29.103
	10	21.235	21.49	21.487	21.701	21.493	32.179	30.24	30.222	30.383	30.222
	100	25.799	26.13	26.147	26.356	26.149	35.379	33.82	33.796	33.960	33.795
	10^6	28.951	28.98	28.951	28.951	28.950	35.992	36.01	35.985	35.987	35.985

Source: a, Ref. [14]; b, Ref. [15]; c, Ref. [16]; d, Ref. [17].

Table 2
Convergence study in terms of frequency parameters, $\Omega = \omega a^2\sqrt{\rho h/D}$, for the CECE square plate with $K_c = 1$.

$M = N$	Ω_1	Ω_2	Ω_3	Ω_4	Ω_5	Ω_6	Ω_7	Ω_8	Ω_9	Ω_{10}
$n = 6$	29.107	55.087	69.393	94.797	102.70	129.21	140.67	155.21	170.94	201.11
$n = 7$	29.103	55.069	69.389	94.796	102.62	129.13	140.58	154.94	170.83	200.15
$n = 8$	29.103	55.067	69.384	94.755	102.62	129.13	140.49	154.92	170.79	200.15
$n = 9$	29.103	55.064	69.383	94.755	102.60	129.12	140.47	154.88	170.77	200.01
$n = 10$	29.103	55.064	69.382	94.748	102.60	129.12	140.46	154.88	170.76	200.01
$n = 11$	29.103	55.064	69.382	94.748	102.60	129.12	140.45	154.87	170.76	199.98

problem with the current method. When the displacement is not identically equal to zero along each edge, the frequency parameter, $\Omega = \omega a^2\sqrt{\rho h/D}$, will become dependent upon Poisson's ratio. For the simplicity, Poisson's ratio will be set as $\nu = 0.3$in the following calculations.

In the current method, the stiffness for each restraining spring can be specified as an arbitrary function of spatial coordinates. Specifically, we will consider the restraining scheme depicted in Fig. 2 where the stiffness functions are "arbitrarily" selected as uniform, linear, parabolic and sinusoidal along the edges. As mentioned earlier, each of the stiffness function will be generally represented by a Fourier cosine series expansion as given in Eq. (25). For convenience, the current restraining conditions at $x = 0$, $y = b$, $x = a$ and $y = 0$ will be labeled as ①, ②, ③ and ④, respectively. Several boundary conditions representing various combinations of these four restraining conditions and free edge will be considered here. The first ten frequency parameters, $\Omega = \omega a^2\sqrt{\rho h/D}$, are presented in Tables 4–6 for plates of different aspect ratios, $r = b/a$, when they are subjected to the restraining condition ① and free at other three edges. When the strength factor k_c is a very large number, 10^6, the boundary condition essentially degenerate into the classical case CFFF. The previous solutions [47] for this particular case are included in Tables 4 and 5 for comparison. Since no result is readily found in the literature for a moderate k_c value, the FEM data is given in Table 6 as a reference solution. In the FEA model, each edge is divided into

Table 3
Frequency parameters, $\Omega = \omega a^2\sqrt{\rho h/D}$, for several cases, in which S means simply supported, C clamped, E simply supported with rotational springs of parabolically varying stiffness.

CASE	Ω_1	Ω_2	Ω_3	Ω_4	Ω_5	Ω_6	Ω_7	Ω_8
ESSC	23.749	51.862	58.695	86.270	100.485	113.262	133.980	140.960
	23.750[a]	51.868	58.685	86.237	100.498	113.254	133.942	140.915
ESCS	23.794	51.742	58.845	86.285	100.313	113.445	133.918	141.041
	23.803[a]	51.728	58.861	86.256	100.296	113.469	133.868	141.012
ECCS	27.181	60.639	60.926	92.960	114.631	114.868	145.877	146.243
	27.192[a]	60.654	60.931	92.957	114.643	114.890	145.912	146.207
ECSC	29.026	54.903	69.354	94.665	102.408	129.108	140.324	154.820
	29.039[a]	54.932	69.365	94.689	102.447	129.131	140.363	154.858
CEES	23.883	51.907	58.877	86.369	100.506	113.460	134.040	141.091
	23.906[a]	51.921	58.897	86.355	100.523	113.488	134.013	141.070
SECE	23.839	52.027	58.727	86.354	100.678	113.278	134.102	141.010
	23.855[a]	52.061	58.721	86.337	100.725	113.272	134.087	140.974

[a] Ref. [17].

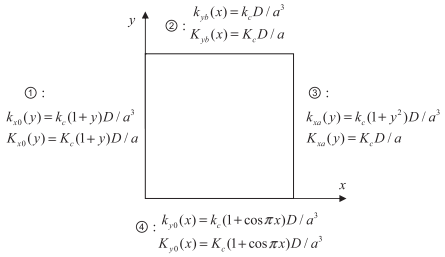

Fig. 2. A rectangular plate with varying elastic edge supports including linear, parabolic, and harmonic functions.

Table 4
Frequency parameters, $\Omega = \omega a^2\sqrt{\rho h/D}$, for rectangular plates with boundary condition ①: $k_{x0}(y) = k_c(1+y)D/a^3$, $K_{x0}(y) = K_c(1+y)D/a$, and free on all other three edges, aspect ratio $r = 1$.

$K_c = k_c$	Ω_1	Ω_2	Ω_3	Ω_4	Ω_5	Ω_6	Ω_7	Ω_8	Ω_9	Ω_{10}
0	0.00	0.00	0.00	13.47	19.60	24.27	34.80	34.80	61.09	61.09
1	1.00	1.24	3.87	13.92	20.85	25.41	35.07	36.12	61.14	63.57
10	2.47	3.53	7.48	15.38	22.16	29.02	36.09	39.22	61.33	66.04
100	3.29	7.13	15.59	21.59	24.12	35.33	39.68	44.02	62.11	68.92
1000	3.18	8.34	20.54	25.04	29.46	40.13	55.15	57.91	61.53	69.69
10^6	3.47	8.51	21.29	27.20	30.96	54.19	61.26	64.14	70.98	92.93
	3.47[a]	8.50	21.28	27.20	30.95	54.19				

[a] Ref. [47].

Table 5
Frequency parameters, $\Omega = \omega a^2\sqrt{\rho h/D}$, for rectangular plates with boundary condition ①: $k_{x0}(y) = k_c(1+y)D/a^3$, $K_{x0}(y) = K_c(1+y)D/a$, and free on all other three edges, aspect ratio $r = 2$.

$K_c = k_c$	Ω_1	Ω_2	Ω_3	Ω_4	Ω_5	Ω_6	Ω_7	Ω_8	Ω_9	Ω_{10}
0	0.00	0.00	0.00	21.46	26.58	58.48	59.61	88.01	101.5	104.0
1	1.01	1.27	3.87	23.82	26.72	58.99	62.30	88.24	102.6	104.1
10	2.47	3.76	7.50	27.43	28.46	60.62	69.34	89.10	104.8	106.3
100	3.27	9.62	15.77	31.65	35.36	63.61	74.44	90.75	108.1	109.8
1000	3.41	13.99	20.76	44.19	54.65	79.67	91.33	97.80	117.9	124.4
10^6	3.44	14.81	21.45	48.19	60.18	92.55	93.10	118.5	126.7	152.8
	3.44[a]	14.80	21.43	48.17	60.14	92.51				

[a] Ref. [47].

Table 6
Frequency parameters, $\Omega = \omega a^2\sqrt{\rho h/D}$, for rectangular plates with boundary condition ① $k_c = K_c = 1$, and free on all other three edges.

$r = a/b$	Ω_1	Ω_2	Ω_3	Ω_4	Ω_5	Ω_6	Ω_7	Ω_8	Ω_9	Ω_{10}
1	1.00	1.24	3.87	13.92	20.85	25.41	35.07	36.12	61.14	63.57
	1.01[a]	1.25	3.89	13.93	20.86	25.42	35.07	36.13	61.14	63.59
1.5	1.00	1.26	3.87	20.33	23.79	47.16	49.96	59.80	67.70	87.43
2	1.01	1.27	3.87	23.82	26.72	58.99	62.30	88.24	102.6	104.1
2.5	1.01	1.29	3.87	23.80	33.09	62.30	71.14	118.9	119.4	140.4
4	1.03	1.44	3.88	23.74	52.21	62.03	108.2	119.8	171.7	197.1

[a] Finite element method with 100×100 elements.

Table 7
Frequency parameters, $\Omega = \omega a^2\sqrt{\rho h/D}$, for rectangular plates with boundary condition ①+③ with $k_c = K_c = 1$, and free on other edges.

$r = a/b$	Ω_1	Ω_2	Ω_3	Ω_4	Ω_5	Ω_6	Ω_7	Ω_8	Ω_9	Ω_{10}
1	1.51	1.84	5.48	14.31	21.40	26.61	35.24	37.13	61.19	64.72
1.5	1.51	1.85	5.48	20.54	25.52	47.79	50.01	61.07	68.38	88.57
2	1.52	1.86	5.48	25.54	26.85	59.38	64.19	88.38	103.5	104.2
2.5	1.54	1.89	5.47	25.52	33.17	64.19	71.39	119.6	121.2	140.4
4	1.60	2.07	5.47	25.44	52.26	63.91	108.3	121.8	171.9	199.1

Table 8
Frequency parameters, $\Omega = \omega a^2\sqrt{\rho h/D}$, for rectangular plates with boundary condition ①+③+④ with $k_c = K_c = 1$, and free at $y = 0$.

$r = a/b$	Ω_1	Ω_2	Ω_3	Ω_4	Ω_5	Ω_6	Ω_7	Ω_8	Ω_9	Ω_{10}
1	1.82	3.80	5.57	14.65	22.92	26.80	36.19	37.30	62.98	65.13
1.5	2.00	5.61	6.27	21.34	25.65	48.12	52.56	62.23	69.19	88.83
2	2.14	5.66	9.43	25.65	28.35	60.03	64.37	91.90	103.8	107.1
2.5	2.27	5.70	13.13	25.63	35.58	64.34	72.50	120.3	121.7	144.5
4	2.59	5.83	25.35	26.97	58.59	64.09	111.5	122.0	173.9	199.3

Table 9
Frequency parameters, $\Omega = \omega a^2\sqrt{\rho h/D}$, for rectangular plates with boundary condition ①+②+③+④ with $k_c = K_c = 1$.

$r = a/b$	Ω_1	Ω_2	Ω_3	Ω_4	Ω_5	Ω_6	Ω_7	Ω_8	Ω_9	Ω_{10}
1	2.17	5.14	5.71	15.00	24.17	27.14	37.17	37.53	64.56	65.48
	2.18[a]	5.09	5.78	14.98	24.17	27.16	37.12	37.50	64.57	65.49
1.5	2.39	5.75	8.78	22.12	25.77	48.46	54.76	63.22	70.21	89.07
2	2.58	5.84	13.24	25.75	29.82	60.68	64.53	94.94	104.3	110.1
2.5	2.76	5.93	18.36	25.73	37.97	64.46	73.60	121.0	122.1	148.0
4	3.23	6.18	25.68	36.85	64.16	64.96	114.7	122.1	175.9	199.6

[a] Finite element method with 100×100 elements.

100 elements, which is considered adequately fine to capture the spatial variations of these lower order modes. The current results match well with those obtained from the FEA model. Usually, the frequency parameters tend to increase with the aspect ratio, as indicated by the results in Table 6 for the fifth modes and higher. Since the first three modes in each case

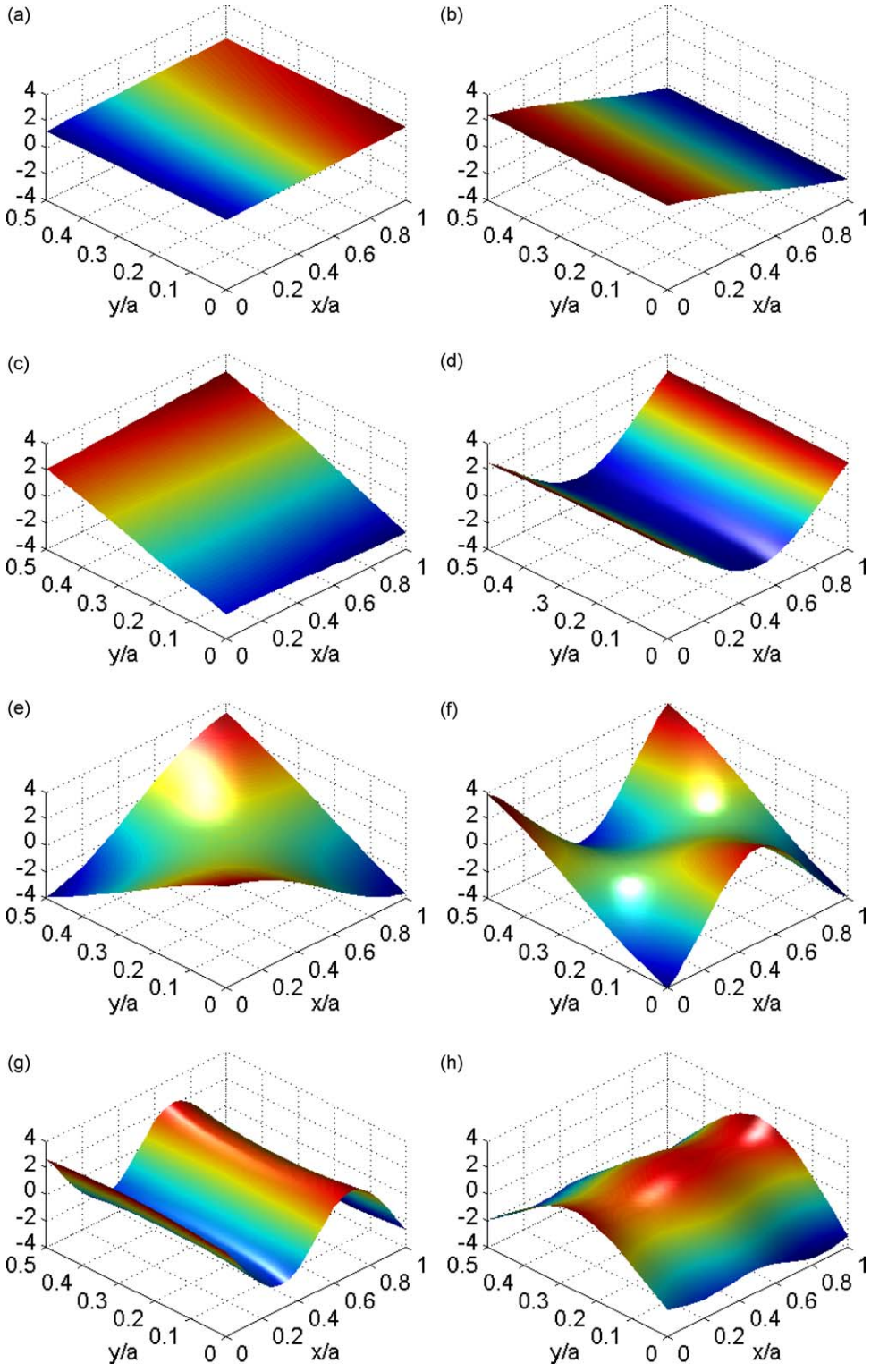

Fig. 3. The mode shapes for a plate of aspect ratio $r = 2$ under the boundary condition: ①+②+③+④. The (a) first, (b) second, (c) third, (d) fourth, (e) fifth, (f) sixth, (g) seventh and (h) eighth mode shape.

basically represent the rigid-body motions, the corresponding frequency parameters are primarily determined by the stiffnesses of elastic restraints at edge $x = 0$, and hence barely affected by the aspect ratio. In comparison, the fourth modes actually represent two different types of flexible modes: a) the twisting like motion of a free plate for $r = 1, 1.5$; and b) the bending-like motion of a free beam for $r = 2, 2.5, 4$. These explain the particular patterns for frequency parameters for the fourth modes in Table 6.

Shown in Tables 7–9 are the frequency parameters for a few more complicated cases when two or more edges are elastically restrained ($k_c = K_c = 1$). It is interesting to note from Table 7 that the first three frequencies are basically unaffected by the aspect ratio (when $r \leqslant 2.5$) for the ①+free+③+free configuration. The FEA results are also given in Table 9 for the combination of ①+②+③+④. Again, a good comparison is observed between these two different solution techniques.

Thus far, our attention has been focused on the frequency parameters for different boundary conditions and aspect ratios. As a matter of fact, in the current solution the eigenpairs (eigenfrequencies and eigenvectors) are simultaneously obtained from the characteristic equation, Eq. (29). For a given eigenfrequency, the corresponding eigenvector actually contains the expansion coefficients, A_{mn}, c_m and d_n from which the mode shape can be readily calculated from Eq. (15) in an analytical form. For example, plotted in Fig. 3 are the first eight mode shapes for a plate of aspect ratio $r = 2$ under the boundary condition of ①+②+③+④. For conciseness, the FEA mode shapes will not be presented here; it suffices to say that the modes in Fig. 3 have all been validated by the FEA model.

4. Conclusions

An analytical method has been developed for the vibration analysis of rectangular plates with arbitrary elastic edge restraints of varying stiffness distributions. The displacement function is generally expressed as a standard two-dimensional Fourier cosine series supplemented by several one-dimensional Fourier series expansions which are introduced to ensure the availability and uniform convergence of the series representation for any boundary conditions. Unlike the existing techniques such as DQ and DSC methods, the current method offers a unified solution to a wide class of plate problems and does not require any special procedures or schemes in dealing with different boundary conditions. Both translational and rotational restraints can be generally specified along any edge, and an arbitrary stiffness distribution is universally described in terms of a set of invariants, cosine functions. While this treatment is very useful and effective for a continuously distributed restraint, it may not be best suitable for a discretely or partially restrained edge because of the possible slow convergence or overshoots of the series representation at or near a discontinuity point. This problem, however, can be easily resolved by substituting the given (discontinuous) stiffness functions into Eq. (21) directly and carrying out the integrations analytically or numerically. The method was first applied to several "classical" cases which were previously investigated by using various techniques. It was also used to solve a class of more difficult problems in which the displacement is no longer completely restrained in the translational direction. The accuracy and reliability of the current method are repeatedly demonstrated through all these examples as evidenced by a good comparison with the existing or FEA results. Although the current solution is sought in a weak form from the Rayleigh–Ritz procedure, it is mathematically equivalent to what would be obtained from the strong formulation because the constructed displacement function is sufficiently smooth over the entire solution domain. The adoption of a weak formulation may become far more advantageous when the vibration of a plate structure is attempted. Finally, it should be mentioned that this Fourier series method is currently being extended to the vibrations of non-rectangular plates including triangular and L-shaped plate.

Acknowledgment

The authors gratefully acknowledge the financial support from NSF Grant: CMMI-0827233.

Appendix A. Supplemental definitions of symbols used in Eqs. (26)–(28)

Let

$$\xi_a^j(x) = s_1^j \sin\left(\frac{\pi x}{2a}\right) + s_2^j \cos\left(\frac{\pi x}{2a}\right) + s_2^j \sin\left(\frac{3\pi x}{2a}\right) + s_4^j \cos\left(\frac{3\pi x}{2a}\right) \tag{A.1}$$

and

$$\xi_b^j(y) = t_1^j \sin\left(\frac{\pi y}{2a}\right) + t_2^j \cos\left(\frac{\pi y}{2a}\right) + t_2^j \sin\left(\frac{3\pi y}{2a}\right) + t_4^j \cos\left(\frac{3\pi y}{2a}\right). \tag{A.2}$$

We then define

$$\alpha_m^j = \int_0^a \xi_a^j(x) \cos \lambda_{am} x \, dx = \sum_{p=1}^{4} s_p^j \tau_{am}^p, \tag{A.3}$$

$$\bar{\alpha}_m^j = \int_0^a \xi_a^{\prime j}(x)\sin\ \lambda_{am}x\,\mathrm{d}x \tag{A.4}$$

$$\bar{\bar{\alpha}}_m^l = \frac{1}{\Delta_m}\int_0^a \xi_a^{\prime\prime j}(x)\cos\ \lambda_{am}x\,\mathrm{d}x = \sum_{p=1}^{4} s_p^l(-\lambda_{ap}^2)\tau_{am}^p, \tag{A.5}$$

$$\beta_n^j = \int_0^b \xi_b^j(y)\cos\ \lambda_{bn}y\,\mathrm{d}y = \sum_{q=1}^{4} t_q^j\kappa_{bn}^q, \tag{A.6}$$

$$\bar{\beta}_n^j = \int_0^b \xi_a^{\prime j}(y)\sin\ \lambda_{bn}y\,\mathrm{d}y \tag{A.7}$$

$$\bar{\bar{\beta}}_n^j = \int_0^b \xi_a^{\prime\prime j}(y)\cos\ \lambda_{bn}y\,\mathrm{d}y = \sum_{q=1}^{4} t_q^j(-\lambda_{bq}^2)\kappa_{bn}^q \tag{A.8}$$

$$\tilde{\alpha}_m^j = \alpha_m^j/\Delta_m, \quad \tilde{k}_{x0,n} = k_{x0,n}/\Delta_n, \quad \tilde{K}_{x0,n} = K_{x0,n}/\Delta_n, \tag{A.9–11}$$

$$\alpha_{i,j}^{0,0} = \int_0^a \xi_{ia}(x)\xi_{ja}(x)\,\mathrm{d}x, \quad \alpha_{i,j}^{0,2} = \int_0^a \xi_{ia}(x)\xi_{ja}^{\prime\prime}(x)\,\mathrm{d}x, \tag{A.12, A.13}$$

$$\alpha_{i,j}^{2,0} = \int_0^a \xi_{ia}^{\prime\prime}(x)\xi_{ja}(x)\,\mathrm{d}x, \quad \alpha_{i,j}^{2,2} = \int_0^a \xi_{ia}^{\prime\prime}(x)\xi_{ja}^{\prime\prime}(x)\,\mathrm{d}x \tag{A.14, A.15}$$

where τ_{am}^p denote the expansion coefficients of the following functions

$$\cos\left(\frac{\pi}{2a}x-\frac{\pi}{2}\right) = \sum_{m=0}^{\infty}\tau_{am}^1\cos\ \lambda_{am}x, \quad \cos\left(\frac{\pi}{2a}x\right) = \sum_{m=0}^{\infty}\tau_{am}^2\cos\ \lambda_{am}x, \tag{A.16, A.17}$$

$$\cos\left(\frac{3\pi}{2a}x-\frac{\pi}{2}\right) = \sum_{m=0}^{\infty}\tau_{am}^3\cos\ \lambda_{am}x, \quad \text{and} \quad \cos\left(\frac{3\pi}{2a}x\right) = \sum_{m=0}^{\infty}\tau_{am}^4\cos\ \lambda_{am}x. \tag{A.18, A.19}$$

More explicitly, they are calculated from

$$\tau_{am}^1 = \begin{cases} m=0 & \dfrac{2}{\pi} \\ m\neq 0 & \dfrac{4}{(1-4m^2)\pi} \end{cases}, \quad \tau_{am}^2 = \begin{cases} m=0 & \dfrac{2}{\pi} \\ m\neq 0 & \dfrac{4(-1)^m}{(1-4m^2)\pi} \end{cases}, \tag{A.20, A.21}$$

$$\tau_{am}^3 = \begin{cases} m=0 & \dfrac{2}{3\pi} \\ m\neq 0 & \dfrac{12}{(9-4m^2)\pi} \end{cases}, \quad \tau_{am}^4 = \begin{cases} m=0 & -\dfrac{2}{3\pi} \\ m\neq 0 & \dfrac{12(-1)^{m+1}}{(9-4m^2)\pi} \end{cases}, \tag{A.22, A.23}$$

$$\bar{\alpha}_m^1 = \frac{m}{\pi}\left(\frac{9}{4m^2-1}-\frac{1}{4m^2-9}\right), \quad \bar{\alpha}_m^2 = (-1)^{m+1}\frac{m}{\pi}\left(\frac{9}{4m^2-1}-\frac{1}{4m^2-9}\right), \tag{A.24, A.25}$$

$$\bar{\alpha}_m^3 = \frac{4ma^2}{\pi^3}\left(\frac{1}{4m^2-1}-\frac{1}{4m^2-9}\right) \quad \text{and} \quad \bar{\alpha}_m^4 = (-1)^{m+1}\frac{4ma^2}{\pi^3}\left(\frac{1}{4m^2-1}-\frac{1}{4m^2-9}\right). \tag{A.26, A.27}$$

The y counterparts, κ_{bn}^q, can be directly obtained from τ_{am}^j by replacing m with n, and a with b in the above equations.

References

[1] A.W. Leissa, Vibration of plates, *Acoustical Society of America*, 1993.

[2] T.E. Carmichael, The vibration of a rectangular plate with edges elastically restrained against rotation, *The Quarterly Journal of Mechanics and Applied Mathematics* 12 (1959) 29–42.

[3] C.V. Joga-Rao, C.L. Kantham, Natural frequencies of rectangular plates with edges elastically restrained against rotation, *Journal of Aeronautical Science* 24 (1957) 855–856.

[4] W.H. Hoppmann, J. Greenspon, an experimental device for obtaining elastic rotational constraints on the boundary of a plate, *Proceedings of the US National Congress of Applied Mechanics*, 1954, pp. 187–191.

[5] P.A.A. Laura, E. Romanelli, Vibration of rectangular plates elastically restrained against rotation along all edges and subjected to a biaxial state of stress, *Journal of Sound and Vibration* 37 (1974) 367–377.

[6] P.A.A. Laura, L.E. Luisoni, C. Filipich, A note on the determination of the fundamental frequency of vibration of thin, rectangular plates with edges possessing different rotational flexibility coefficients, *Journal of Sound and Vibration* 55 (1977) 327–333.
[7] P.A.A. Laura, L.E. Luisoni, G. Ficcadenti, On the effect of different edge flexibility coefficients on transverse vibration of thin rectangular plates, *Journal of Sound and Vibration* 57 (1978) 333–340.
[8] P.A.A. Laura, R. Grossi, Transverse vibration of a rectangular plate elastically restrained against rotation along three edges and free on the fourth edge, *Journal of Sound and Vibration* 59 (1978) 355–368.
[9] P.A.A. Laura, R.O. Grossi, S.R. Soni, Free vibration of a rectangular plate of variable thickness elastically restrained against rotation along three edges and free on the fourth edge, *Journal of Sound and Vibration* 62 (1979) 493–503.
[10] D.M. Egle, The response of a rectangular plate with an elastic edge restraint, *ASME Journal of Engineering for Industry* 94 (1972) 517–525.
[11] E.E.M. Nassar, On the dynamic characteristics of beams, plates, and shells, PhD Thesis, Georgia Institute of Technology, 1973.
[12] W.L. Li, M. Daniels, A Fourier series method for the vibrations of elastically restrained plates arbitrarily loaded with springs and masses, *Journal of Sound and Vibration* 252 (2002) 768–781.
[13] W.L. Li, Vibration analysis of rectangular plates with general elastic boundary supports, *Journal of Sound and Vibration* 273 (2004) 619–635.
[14] A.W. Leissa, P.A.A. Laura, R.H. Gutierrez, Vibration of rectangular plates with non-uniform elastic edge supports, *Journal of Applied Mechanics* 47 (1979) 891–895.
[15] P.A.A. Laura, R.H. Gutierrez, Analysis of vibrating rectangular plates with nonuniform boundary conditions by using the differential quadrature method, *Journal of Sound and Vibration* 173 (1994) 702–706.
[16] C. Shu, C.M. Wang, Treatment of mixed and nonuniform boundary conditions in GDQ vibration analysis of rectangular plates, *Engineering Structures* 21 (1999) 125–134.
[17] Y.B. Zhao, G.W. Wei, DSC analysis of rectangular plates with non-uniform boundary conditions, *Journal of Sound and Vibration* 255 (2002) 203–228.
[18] M.S. Cheung, Finite Strip Analysis of Structures, PhD Thesis, University of Calgary, 1971.
[19] D.J. Gorman, A comprehensive study of the free vibration of rectangular plates resting on symmetrically-distributed uniform elastic edge supports, *Journal of Applied Mechanics* 56 (1980) 893–899.
[20] C. Shu, A generalized approach for implementing general boundary conditions in the GDQ free vibration analysis of plates, *International Journal of Solids Structures* 34 (1997) 837–846.
[21] G.W. Wei, Y.B. Zhao, Y. Xiang, The determination of natural frequencies of rectangular plates with mixed boundary conditions by discrete singular convolution, *International Journal of Mechanical Sciences* 43 (2001) 1731–1746.
[22] R. Bellman, Differential quadrature and long-term integration, *Journal of Mathematical Analysis and Applications* 34 (1971) 235–238.
[23] R. Bellman, B.G. Kashef, J. Casti, Differential quadrature: a technique for the rapid solution of nonlinear partial differential equations, *Journal of Computational Physics* 10 (1972) 40–52.
[24] C.W. Bert, X. Wang, A.G. Striz, Convergence of the DQ method in the analysis of anisotropic plates, *Journal of Sound and Vibration* 170 (1994) 140–144.
[25] G.W. Wei, Discrete singular convolution for the solution of the Fokker–Planck equation, *Journal of Chemical Physics* 110 (1999) 8930–8942.
[26] S. Zhao, G.W. Wei, Y. Xiang, DSC analysis of free-edged beams by an iteratively matched boundary method, *Journal of Sound and Vibration* 284 (2005) 487–493.
[27] D.J. Gorman, Free vibration and buckling of in-plane loaded plates with rotational elastic edge support, *Journal of Sound and Vibration* 225 (2000) 755–773.
[28] D.J. Gorman, Free vibration analysis of corner-supported rectangular plates with symmetrically distributed edge beams, *Journal of Sound and Vibration* 263 (2003) 979–1003.
[29] D.J. Gorman, Free vibration analysis of Mindlin plates with uniform elastic edge support by the superposition method, *Journal of Sound and Vibration* 207 (1997) 335–350.
[30] G.B. Warburton, The vibrations of rectangular plates, *Proceedings of the Institute of Mechanical Engineers, Series A* 168 (1954) 371–384.
[31] A.W. Leissa, The free vibrations of rectangular plates, *Journal of Sound and Vibration* 31 (1973) 257–293.
[32] S.M. Dickinson, E.K.H. Li, On the use of simply supported plate functions in the Rayleigh–Ritz method applied to the vibration of rectangular plates, *Journal of Sound and Vibration* 80 (1982) 292–297.
[33] G.B. Warburton, Response using the Rayleigh–Ritz method, *Journal of Earthquake Engineering and Structural Dynamics* 7 (1979) 327–334.
[34] G.B. Warburton, S.L. Edney, Vibrations of rectangular plates with elastically restrained edges, *Journal of Sound and Vibration* 95 (1984) 537–552.
[35] P.A.A. Laura, R.O.G. Grossi, Transverse vibration of rectangular plates with edges elastically restrained against translation and rotation, *Journal of Sound and Vibration* 75 (1981) 101–107.
[36] P. Cupial, Calculation of the natural frequencies of composite plates by the Rayleigh–Ritz method with orthogonal polynomials, *Journal of Sound and Vibration* 201 (1997) 385–387.
[37] R.B. Bhat, Natural frequencies of rectangular plates using characteristic orthogonal polynomials in the Rayleigh–Ritz method, *Journal of Applied Mechanics* 102 (1985) 493–499.
[38] S.M. Dickinson, A. Di-Blasio, On the use of orthogonal polynomials in the Rayleigh–Ritz method for the flexural vibration and buckling of isotropic and orthotropic rectangular plates, *Journal of Applied Mechanics* 108 (1986) 51–62.
[39] P.A.A. Laura, Comments on "Natural frequencies of rectangular plates using a set of static beam functions in the Rayleigh–Ritz method," *Journal of Sound and Vibration* 200 (1997) 540–542.
[40] D. Zhou, Natural frequencies of elastically restrained rectangular plates using a set of static beam functions in the Rayleigh–Ritz method, *Computers & Structures* 57 (1995) 731–735.
[41] D. Zhou, Natural frequencies of rectangular plates using a set of static beam functions in the Rayleigh–Ritz method, *Journal of Sound and Vibration* 189 (1996) 81–88.
[42] O. Beslin, J. Nicolas, A hierarchical functions sets for very high-order plate bending modes with any boundary conditions, *Journal of Sound and Vibration* 202 (1997) 633–655.
[43] S. Hurlebaus, L. Gaul, J.T.-S. Wang, An exact solution for calculating the eigenfrequencies of orthotropic plates with completely free boundary, *Journal of Sound and Vibration* 244 (2001) 747–759.
[44] M.B. Rosales, C.P. Filipich, Vibration of orthotropic plates: discussion on the completeness of the solutions used in direct methods, *Journal of Sound and Vibration* 261 (2003) 751–757.
[45] C.P. Filipich, M.B. Rosales, Arbitrary precision frequencies of a free rectangular thin plate, *Journal of Sound and Vibration* 230 (2000) 521–539.
[46] J.T. Du, W.L. Li, G.Y. Jin, T.J. Yang, Z.G. Liu, An analytical method for the in-plane vibration analysis of rectangular plates with elastically restrained edges, *Journal of Sound and Vibration* 306 (2007) 908–927.
[47] W.L. Li, X.F. Zhang, J.T. Du, Z.G. Liu, An exact series solution for the transverse vibration of rectangular plates with general elastic boundary supports, *Journal of Sound and Vibration* 321 (2009) 254–269.
[48] W.L. Li, Free vibration of beams with general boundary conditions, *Journal of Sound and Vibration* 237 (2000) 709–725.